Inelastic X-Ray Scattering from Shocked Liquid Deuterium

Extreme states of matter existing in astrophysical objects (e.g., stars and planetary interiors) can be created in the laboratory with high-intensity laser beams, particle beams, and *Z*-pinch generators.[1] High-energy-density physics (HEDP) encompasses the research of matter having energy densities of ~10^{11} J/m^3 or more or, equivalently, pressures greater than 1 Mbar (Refs. 1 and 2). A subset of this field involves the study of warm, dense matter (WDM)[1,2] with electron temperatures around the Fermi temperature and the ratio of the potential energy to the kinetic energy of the ions greater than unity. The latter can be quantified by an ion–ion coupling parameter[2] $\Gamma_{ii} = (Ze)^2 \big/ d_i k_B T > 1$, where Ze is the electric charge of the ion, d_i is the mean ion spacing, k_B is the Boltzmann constant, and T is the temperature. In shock-compressed matter at these extreme conditions, the determination of the system properties, in particular the equation of state (EOS), is complicated by the highly correlated nature of the medium, consisting of a system of strongly coupled ions immersed in a fluid of partially degenerate electrons. Understanding the physical properties (e.g., opacity,[3] conductivity,[4] EOS,[5] and compressibility[6]) of WDM is, however, very important for inertial confinement fusion (ICF) research[7,8] and the study of planetary interiors[9] because theoretical models differ by factors of several when predicting these quantities. In the past decade, developments in laser-produced plasma sources and detector efficiencies have made inelastic x-ray scattering a powerful diagnostic providing electron temperature (T_e), electron density (n_e), and ionization (Z) for critical EOS measurements in ICF and planetary science research.[10–14]

This article describes the first experimental observation of noncollective, inelastic x-ray Thomson scattering from liquid deuterium driven by a laser-produced ~10-Mbar shock wave. The average electron temperature, electron density, and ionization are inferred from spectral intensity of the elastic (Rayleigh) and inelastic (Compton) components of the scattered Cl Ly$_\alpha$ emission at 2.96 keV. Two-dimensional (2-D) hydrodynamic simulations using EOS models designed for the extreme conditions found in ICF research and planetary interiors predict an average state of the plasma that is consistent with the x-ray scattering measurements.

The EOS of hydrogen for pressures <10 Mbar along the Hugoniot remains uncertain,[15–17] where detailed validation of experimental techniques and numerical modeling is of utmost importance. While the present work has not obtained density measurements with accuracy below a few percent, it provides a needed alternative experimental platform where such validation could take place. The reason is twofold: X-ray scattering experiments at near solid densities or above ($n_e > 10^{22}$ cm^{-3}) have been successfully performed at laser facilities[10] because of the high initial density. In the case of deuterium, as described here, a significant technological advance was necessary to observe the x-ray Thomson scattering with the development of dedicated cryogenic target hardware for the x-ray scattering experimental platform. This allowed liquid deuterium to be shock heated to reach densities comparable to previous x-ray scattering experiments. Since an elastic scattering cross section goes as Z^2, cryogenic liquid deuterium scatters significantly less x rays than previous experiments using room-temperature solids. To overcome the reduction in scattering fraction and achieve a reasonable signal-to-noise ratio, a target geometry with a large collection volume inside the cryogenic cell was adopted for this proof-of-principle experiment at a cost of spatial resolution and accuracy in the density measurements.

This research provides an experimental platform for the detailed study of compressed deuterium and is an important step toward measuring all the thermodynamic variables needed for EOS research, i.e., pressure (p), mass density (ρ), electron density (n_e), electron temperature (T_e), and ionization (Z), by combining inelastic x-ray scattering with shock-velocity and optical pyrometry measurements.[5,15–17]

The platform to measure the spectrally resolved inelastic x-ray scattering from shocked deuterium was developed on the 60-beam, 30-kJ, 351-nm OMEGA Laser System.[18] Inelastic x-ray scattering is predominantly collective or noncollective, depending on the scattering parameter $\alpha_s = 1/k\lambda_s$, where the wave number of the scattered x ray is given by $k = 4\pi/\lambda_0 \sin(\theta/2)$ with the incident wavelength $\lambda_0 = 4.188$ Å, λ_s is electron screening length of the plasmas, and θ is the scattering angle. For the

partially ionized conditions in WDM, the screening length may be calculated from the Fermi distribution via a single integral.[19] An easier fourth-order interpolation between the classical Debye length and the Thomas–Fermi screening length valid for $T = 0$ yields the correct results within 2% (Ref. 19). If $\alpha_s < 1$, the scattering is dominated by independent electrons and is referred to as noncollective.[12] In this case, the free-electron contribution experiences a significant Compton shift $\Delta E_C = \hbar^2 k^2 / 2m_e$ and is Doppler broadened. The width of this scattering feature is sensitive to the electron temperature for nondegenerate plasmas. If $\alpha_s \gg 1$, the scattering by the collective modes, which are known as plasma waves or plasmons, is dominant and the scattering is referred to as collective.[2,10] To lowest order, the position of the energy-downshifted plasmon feature is related to the electron plasma frequency $\omega_{pe} = \sqrt{n_e e^2 / \varepsilon_0 m_e}$, providing an electron-density diagnostic. The Compton downshift for this experiment is 16.5 eV, and the plasma conditions and scattering geometry result in a scattering parameter of $\alpha_s \sim 1$. Since the electrons are partially degenerate, this implies that this inelastic scattering geometry is sensitive to both electron density and temperature, which is a novel regime for inelastic x-ray scattering.[10] Additional information on the plasma temperature is given by the height of the elastic scattering feature.[20]

The experimental setup is shown in Fig. 131.6(a). The 8-μm-thick plastic ablator containing a planar layer of liquid

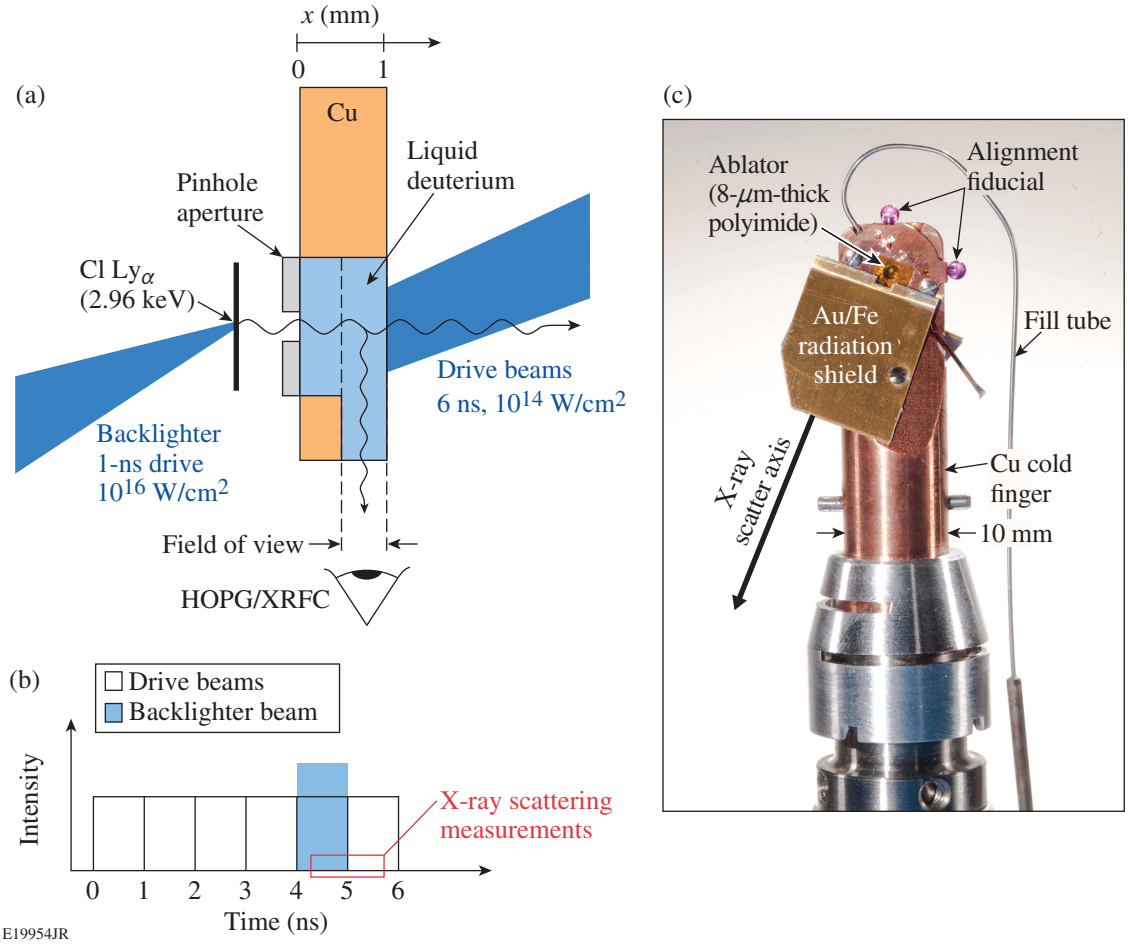

Figure 131.6

(a) Schematic of the x-ray Thomson-scattering (XRTS) experiment. An 8-μm CH ablator was irradiated with a constant-intensity, 6-ns UV laser drive, launching a shock wave through a cryogenic cell filled with liquid deuterium and creating warm, dense matter. Sixteen tightly focused beams irradiated a parylene D backlighter at 10^{16} W/cm^2, producing Cl Ly$_\alpha$ emission; this was scattered at ~90° and detected with an x-ray framing camera outfitted with a HOPG (highly oriented pyrolytic graphite) crystal spectrometer. (b) Timing of the drive and backlighter beams and the x-ray scattering measurements. (c) Photograph of the cryogenic XRTS target. The fill tube directs deuterium gas into the cryogenic cell, where it condenses into liquid. The ruby tooling balls on the top and right side of the Cu cold finger are target-alignment fiducials. The Au/Fe shield blocks a direct line of sight between the laser-produced plasmas and the detector, which is positioned ~90° to the laser drive axis.

deuterium was irradiated with a constant-intensity UV laser drive with 10^{14} W/cm^2. The laser drive, formed with six pairs of beams staggered in time as shown in Fig. 131.6(b), was uniform over a 0.5-mm diameter. Each laser beam was smoothed with a phase plate, producing a super-Gaussian spatial-intensity profile $I(r) = I_0 \exp\left[-(r/\delta)^n\right]$, with a 1/$e$ half-width $\delta = 438$ μm and super-Gaussian power $n = 4.5$. A laser-ablation–driven shock wave was launched through the liquid deuterium, creating warm, dense compressed matter. Sixteen tightly focused beams irradiated a parylene D backlighter with 10^{16} W/cm^2, generating a source of Cl Ly$_\alpha$ emission ($\lambda_0 = 4.188$ Å, $h\nu = 2960$ eV) (Ref. 21). These x rays were then scattered at $\theta = 87.8°$ from the shocked liquid deuterium and detected with an x-ray framing camera (XRFC) outfitted with a highly oriented pyrolytic graphic (HOPG) crystal spectrometer.[22] The backlighter x rays were collimated with a 200-μm-diam pinhole. The timing of the backlighter beams is shown in Fig. 131.6(b). The integration time of the x-ray scattering measurements is ~0.25 ns. A photograph of the cryogenic target with x-ray Thomson scattering (XRTS) capabilities mounted on the OMEGA planar cryogenic system is shown in Fig. 131.6(c), with the main components highlighted. The fill tube directs deuterium gas into the cryogenic cell, where it condenses into liquid. The ruby tooling balls on the top and right side of the Cu cold finger structure are target alignment fiducials. The Au/Fe shield blocks a direct line of sight between the laser-produced plasmas and the detector, which is positioned ~90° to the laser drive axis.

Two-dimensional hydrodynamic simulations of the experiment were performed with the *DRACO* code, which uses the *SESAME* EOS, a three-dimensional (3-D) laser ray trace model that calculates the laser absorption via inverse bremsstrahlung, a flux-limited thermal-transport approximation with a flux limiter of 0.06, and a multigroup diffusion radiation transport approximation using opacity tables created for astrophysics.[23] The simulation results shown in Fig.131.7, with the laser irradiation side and the location of the Cu wall indicated, predict at peak compression a mass density of $\rho \sim 0.8$ g/cm^3, a temperature of $T_e \sim 5$ to 15 eV, and an ionization stage of $Z \sim 0.5$ to 0.8 for the shocked liquid deuterium 5 ns after the drive beams were incident on the target ($t = 5$ ns). The shock front was predicted to have advanced ~375 μm at $t = 5$ ns and the shocked liquid deuterium had a compressed thickness of ~90 μm. As seen in Fig. 131.7, the spatial-intensity profile of the laser drive creates a curved shock front. The uniformly shocked liquid deuterium region occurs within $r < 0.25$ mm (see Fig. 131.7), and the underdriven shocked liquid deuterium is located at $r >$ 0.25 mm. The predicted plasma conditions in the underdriven shocked portion of the target are lower than the uniform drive portion. The measured spectrum of the scattered x rays is spatially integrated and weighted to the shocked liquid deuterium region, which has the highest density. The field of view of the x-ray scattering channel either extends from $z = 0.5$ mm to $z =$ 1.0 mm (see horizontal scale in Fig. 131.7) or is reduced to $z =$ 0.5 mm to $z = 0.75$ mm by positioning a 250-μm-wide slit in

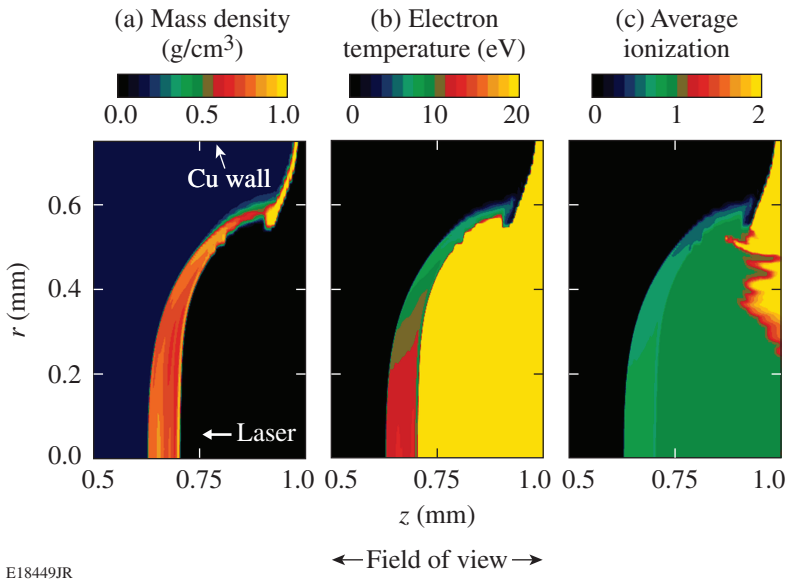

Figure 131.7
Contour plots of (a) mass density, (b) electron temperature, and (c) average ionization of shocked liquid deuterium at 5 ns, predicted using *DRACO*.

the scattering channel. The slit reduces the field of view of the scattering diagnostic to primarily the portion of the shocked liquid deuterium with uniform plasma conditions and blocks the scattering signal from the underdriven portion of the target.

The estimated number N of detected scattered photons[24] is calculated using

$$N = \left(\frac{E_T \eta_T}{h\nu}\right)\left(\frac{\Omega_T}{4\pi}\right)\left(\frac{n_e \sigma_T x}{\alpha_s^2 + 1}\right)\left(\frac{\Omega_x R}{4\pi}\right)\eta_d,$$

where, E_T = 8 kJ is the total UV laser energy incident on the parylene D backlighter foil, η_T = 0.003 is the UV to Cl Ly$_\alpha$ emission conversion efficiency, $h\nu$ = 2.96 keV is the backlighter photon energy, Ω_T = 0.06 steradian is the solid angle of the backlighter plasma sampled by the pinhole, $n_e = 2.2 \times 10^{23}$ cm^{-3} is the electron density of the shocked liquid deuterium, σ_T = 6.6525×10^{-25} cm^2 is the Thomson-scattering cross section, x = 90 μm is the thickness of the shocked liquid deuterium, α_s = 1.3 is the scattering parameter, Ω_x = 0.02 rad is the angle subtended by the detector in the direction perpendicular to the plane of dispersion, R = 3 mrad is the integrated reflectivity of the HOPG Bragg crystal, and η_d = 0.01 is the detector efficiency including filter transmissions. For a sampling time of ~0.25 ns, the total number of detected photons is $N \sim 700$. The thickness of the shocked liquid deuterium is an order of magnitude smaller than the radiatively heated Be targets studied in earlier XRTS experiments;[11,14] consequently, the number of scattered photons in the shocked liquid deuterium experiment is at least an order of magnitude less than the Be experiment.

The scattered spectrum of the Cl Ly$_\alpha$ emission taken at t = 5 ns with a 250-μm slit in the scattering channel is shown in Fig. 131.8(a). The measurement taken without the slit is shown in Fig. 131.8(b), and the incident spectrum is shown in Fig. 131.8(c). The observed noise in the measured scattered x-ray spectrum is consistent with the estimated signal level. The incident spectrum is measured by irradiating a parylene D foil target on a separate laser shot. The scattered spectrum has a strong Rayleigh peak around 2960 eV and a Compton-downshifted feature. Scattered x-ray spectra were calculated using the x-ray scattering (XRS) code, which uses the finite-temperature random-phase approximation with static local field corrections to obtain the spectral shape of the inelastic (Compton) feature caused by scattering from free electrons.[25] The elastic scattering intensity strongly depends on the degree of ion–ion correlations in the plasma via the structure factor S_{ii} (Ref. 20). To constrain the value for S_{ii}, density functional theory molecular dynamics (DFT-MD) simulations were performed using the VASP package.[26,27] The simulations indicate weak ionic correlations for the conditions similar to the average of the plasma probed. This means the ion–ion structure factor S_{ii} at the relevant scattering wave number is close to unity for

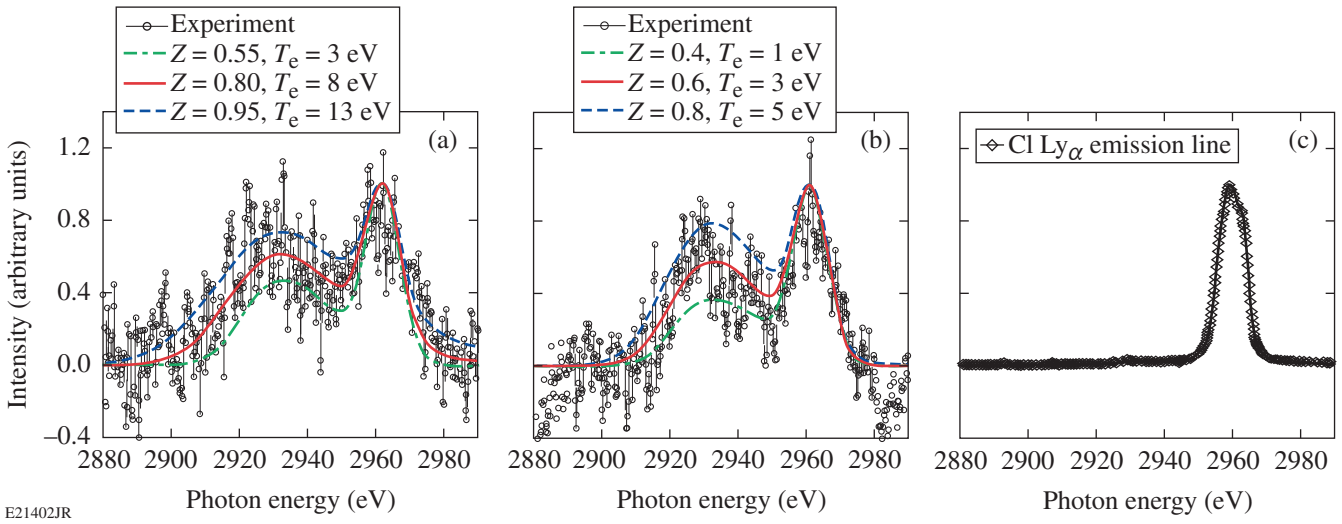

Figure 131.8
Measurement of (a) Cl Ly$_\alpha$ emission scattered from shocked liquid deuterium with a 250-μm slit in the scattering channel and simulated scattering spectra; (b) Cl Ly$_\alpha$ emission scattered from shocked liquid deuterium without a 250-μm slit in the scattering channel and simulated scattering spectra; and (c) Cl Ly$_\alpha$ emission incident on the shocked liquid deuterium. The inferred plasma conditions in (a) are $T_e = 8 \pm 5$ eV, $Z \sim 0.8$ (–0.25, +0.15), and $n_e = 2.2(\pm 0.5) \times 10^{23}$ cm^{-3} and in (b) are $T_e = 3 \pm 2$ eV, $Z \sim 0.6 \pm 0.2$, and $n_e = 2.0(\pm 0.5) \times 10^{23}$ cm^{-3}.

most of the conditions probed. With this information, the elastic scattering feature can be used to constrain the temperature and the ionization degree of the system. Structure factors close to unity are also found for the unshocked deuterium liquid. In addition to Doppler broadening, the width and position of the inelastic feature depend on the density for $\alpha_s \sim 1$. This fact allows us to bracket the electron density and estimate the ionization charge based on the initial mass density of the sample. The simulated scattering spectra computed using XRS provided the best fit to the spectrum measured with the slit for the following plasma conditions: $T_e = 8\pm5$ eV, $Z \sim 0.8$ (–0.25, +0.15), and $n_e = 2.2(\pm0.5) \times 10^{23}$ cm^{-3}. The *DRACO* simulations are in close agreement with the experimental results. These plasma conditions were repeatable on a subsequent laser shot. The plasma conditions inferred from the spectrally resolved x-ray spectrum recorded without the slit in the x-ray scattering channel are lower with $T_e = 3\pm2$ eV, $Z \sim 0.6\pm0.2$, and $n_e = 2.0(\pm0.5) \times 10^{23}$ cm^{-3}. The lower plasma pressure created by the lower-intensity portion of the laser drive causes the bowing of the shock front, as observed in Fig. 131.7. When the slit is placed in the scattering channel, the x rays scattered from this underdriven portion of the target are blocked from the detector. This leads to higher inferred values of T_e, Z, and n_e more representative of the uniformly shocked region.

In conclusion, this article reports the first experimental observation of noncollective, inelastic x-ray scattering from shocked liquid deuterium. An electron temperature of $T_e = 8\pm5$ eV, ionization $Z \sim 0.8$ (–0.25, +0.15), and electron density $n_e = 2.2(\pm0.5) \times 10^{23}$ cm^{-3} are inferred from the shapes and intensities of the elastic (Rayleigh) and inelastic (Compton) components in the scattering spectra. These plasma conditions are Fermi degenerate with similar electron and Fermi temperatures $\left(T_e / T_F \sim 1\right)$. Two-dimensional hydrodynamic simulations using EOS models suited for the extreme conditions indicate that the predicted average state of the probed plasma are consistent with the x-ray scattering measurements. Differently from previous VISAR measurements, the x-ray scattering experimental platform offers the considerable advantage of probing off-Hugoniot states. This experimental result is a significant step toward achieving accurate measurements of all thermodynamic variables needed to provide stringent tests of EOS models, which would require at least three thermodynamic variables like pressure, mass density, and temperature.

ACKNOWLEDGMENT

The authors acknowledge the excellent support of the OMEGA Laser System team, especially M. J. Bonino, R. Earley, S. G. Noyes, D. Turner, K. Lintz, and D. R. Harding. The work of K. F., C. D. M., and G. G. was funded by EPSRC grant no. EP/G007187/1 and by the HiPER fund. The work of J. V. and D. O. G. was partially funded by EPSRC grant no. EP/D062837. This work was supported by the U.S. Department of Energy Office of Inertial Confinement Fusion under Cooperative Agreement No. DE-FC52-08NA28302, the University of Rochester, and the New York State Energy Research and Development Authority. This work was performed under the auspices of the U.S. Department of Energy by Lawrence Livermore National Laboratory under Contract DE-AC52-07NA27344. The support of DOE does not constitute and endorsement by DOE of the views expressed in this article.

REFERENCES

1. National Research Council (U.S.) Committee on High Energy Density Plasma Physics, *Frontiers in High Energy Density Physics: The X-Games of Contemporary Science* (National Academies Press, Washington, DC, 2003).
2. S. Ichimaru, Rev. Mod. Phys. **54**, 1017 (1982).
3. J. E. Bailey *et al*., Phys. Rev. Lett. **99**, 265002 (2007).
4. K. Widmann *et al*., Phys. Rev. Lett. **92**, 125002 (2004).
5. J. Eggert, S. Brygoo, P. Loubeyre, R. S. McWilliams, P. M. Celliers, D. G. Hicks, T. R. Boehly, R. Jeanloz, and G. W. Collins, Phys. Rev. Lett. **100**, 124503 (2008).
6. S. X. Hu, V. A. Smalyuk, V. N. Goncharov, J. P. Knauer, P. B. Radha, I. V. Igumenshchev, J. A. Marozas, C. Stoeckl, B. Yaakobi, D. Shvarts, T. C. Sangster, P. W. McKenty, D. D. Meyerhofer, S. Skupsky, and R. L. McCrory, Phys. Rev. Lett. **100**, 185003 (2008).
7. R. L. McCrory, D. D. Meyerhofer, R. Betti, R. S. Craxton, J. A. Delettrez, D. H. Edgell, V. Yu Glebov, V. N. Goncharov, D. R. Harding, D. W. Jacobs-Perkins, J. P. Knauer, F. J. Marshall, P. W. McKenty, P. B. Radha, S. P. Regan, T. C. Sangster, W. Seka, R. W. Short, S. Skupsky, V. A. Smalyuk, J. M. Soures, C. Stoeckl, B. Yaakobi, D. Shvarts, J. A. Frenje, C. K. Li, R. D. Petrasso, and F. H. Séguin, Phys. Plasmas **15**, 055503 (2008).
8. J. D. Lindl *et al*., Phys. Plasmas **11**, 339 (2004).
9. D. Saumon and G. Chabrier, Phys. Rev. A **44**, 5122 (1991).
10. S. H. Glenzer and R. Redmer, Rev. Mod. Phys. **81**, 1625 (2009).
11. S. H. Glenzer *et al*., Phys. Rev. Lett. **90**, 175002 (2003).
12. G. Gregori *et al*., Phys. Rev. E **67**, 026412 (2003).
13. H. Sawada, S. P. Regan, D. D. Meyerhofer, I. V. Igumenshchev, V. N. Goncharov, T. R. Boehly, R. Epstein, T. C. Sangster, V. A. Smalyuk, B. Yaakobi, G. Gregori, S. H. Glenzer, and O. L. Landen, Phys. Plasmas **14**, 122703 (2007).
14. S. H. Glenzer *et al*., Phys. Rev. Lett. **98**, 065002 (2007).
15. G. W. Collins *et al*., Science **281**, 1178 (1998).
16. P. M. Celliers *et al*., J. Appl. Phys. **98**, 113529 (2005).
17. K. Falk, S. P. Regan, J. Vorberger, M. A. Barrios, T. R. Boehly, D. E. Fratanduono, S. H. Glenzer, D. G. Hicks, S. X. Hu, C. D. Murphy, P. B.

Radha, S. Rothman, A. P. Jephcoat, J. S. Wark, D. O. Gericke, and G. Gregori, High Energy Density Phys. **8**, 76 (2012).

18. T. R. Boehly, D. L. Brown, R. S. Craxton, R. L. Keck, J. P. Knauer, J. H. Kelly, T. J. Kessler, S. A. Kumpan, S. J. Loucks, S. A. Letzring, F. J. Marshall, R. L. McCrory, S. F. B. Morse, W. Seka, J. M. Soures, and C. P. Verdon, Opt. Commun. **133**, 495 (1997).
19. D. O. Gericke *et al*., Phys. Rev. E **81**, 065401(R) (2010).
20. E. García Saiz *et al*., Nat. Phys. **4**, 940 (2008).
21. M. K. Urry *et al*., J. Quant. Spectrosc. Radiat. Transf. **99**, 636 (2006).
22. A. Pak *et al*., Rev. Sci. Instrum. **75**, 3747 (2004).
23. P. B. Radha, V. N. Goncharov, T. J. B. Collins, J. A. Delettrez, Y. Elbaz, V. Yu. Glebov, R. L. Keck, D. E. Keller, J. P. Knauer, J. A. Marozas, F. J. Marshall, P. W. McKenty, D. D. Meyerhofer, S. P. Regan, T. C. Sangster, D. Shvarts, S. Skupsky, Y. Srebro, R. P. J. Town, and C. Stoeckl, Phys. Plasmas **12**, 032702 (2005).
24. O. L. Landen *et al*., J. Quant. Spectrosc. Radiat. Transf. **71**, 465 (2001).
25. G. Gregori *et al*., High Energy Density Phys. **3**, 99 (2007).
26. G. Kresse and J. Furthmüller, Phys. Rev. B **54**, 11169 (1996).
27. J. Vorberger *et al*., Phys. Rev. B **75**, 024206 (2007).